Journal Pre-proof

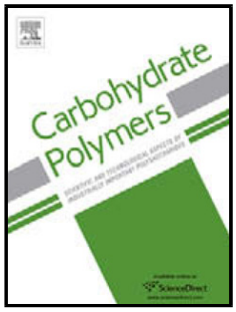

Synthesis of carboxymethyl chitosan-functionalized graphene nanomaterial for anticorrosive reinforcement of waterborne epoxy coating

Hongyi Shi (Methodology) (Writing - original draft) (Writing - review and editing), Weiqu Liu (Project administration) (Supervision), Yankun Xie (Formal analysis) (Resources), Maiping Yang (Data curation) (Investigation), Chunhua Liu (Data curation), Fengyuan Zhang (Resources), Shuo Wang (Validation), Liyan Liang (Project administration) (Supervision), Ke Pi (Investigation)

PII: S0144-8617(20)31422-3

DOI: https://doi.org/10.1016/j.carbpol.2020.117249

Reference: CARP 117249

To appear in: *Carbohydrate Polymers*

Received Date: 24 July 2020

Revised Date: 11 October 2020

Accepted Date: 12 October 2020

Please cite this article as: Shi H, Liu W, Xie Y, Yang M, Liu C, Zhang F, Wang S, Liang L, Pi K, Synthesis of carboxymethyl chitosan-functionalized graphene nanomaterial for anticorrosive reinforcement of waterborne epoxy coating, *Carbohydrate Polymers* (2020), doi: https://doi.org/10.1016/j.carbpol.2020.117249

This is a PDF file of an article that has undergone enhancements after acceptance, such as the addition of a cover page and metadata, and formatting for readability, but it is not yet the definitive version of record. This version will undergo additional copyediting, typesetting and review before it is published in its final form, but we are providing this version to give early visibility of the article. Please note that, during the production process, errors may be discovered which could affect the content, and all legal disclaimers that apply to the journal pertain.

© 2020 Published by Elsevier.

Journal Pre-proof

Synthesis of carboxymethyl chitosan-functionalized graphene nanomaterial for anticorrosive reinforcement of waterborne epoxy coating

Hongyi Shi[a,b], Weiqu Liu[a,b,c,d,e*], Yankun Xie[a,b,d], Maiping Yang [a,b,c,d], Chunhua Liu[a,b,c,d], Fengyuan Zhang[a, b, e], Shuo Wang[a,b,c,d], Liyan Liang[a,b,c,d,e*] and Ke Pi[a,c,d,e]

[a]Guangzhou Institute of Chemistry, Chinese Academy of Sciences, Guangzhou 510650, China

[b]University of Chinese Academy of Sciences, Beijing 100049, China

[c]Guangdong Provincial Key Laboratory of Organic Polymer Materials for Electronics, Guangzhou 510650, China

[d]CASH GCC (Nanxiong) Research Institute of New Materials Co., Ltd, Nanxiong 512400, China

[e]CAS Engineering Laboratory for Special Fine Chemicals, Guangzhou 510650, China

*Corresponding author:

E-mail: liuwq@gic.ac.cn; lyliang@gic.ac.cn;

Postal address: Prof. Weiqu Liu, Prof. Liyan Liang, Guangzhou Institute of Chemistry, Chinese Academy of Sciences, Guangzhou 510650, China

Tel.: +86-20-85231269

Fax: +86-20-85231269

Highlights

Journal Pre-proof

Journal Pre-proof

- Reduced graphene oxide (rGO) was modified by carboxymethyl chitosan (CMCS).
- CMCS-rGO was used as anticorrosive nanofiller for waterborne epoxy (EP) coatings.
- The CMCS-rGO/EP nanocomposites were successfully fabricated and analyzed.
- The dispersion state of rGO in EP matrix was improved after CMCS modification.
- The 0.2 wt% CMCS-rGO/EP nanocomposite exhibitd better anti-corrosion properties.

ABSTRACT

In this study, a carboxymethyl chitosan functionalized graphene (CMCS-rGO) nanomaterial was successfully synthesized in aqueous solution by non-covalent functionalization method. Fourier transform infrared, Raman, ultraviolet visible spectroscopy and thermogravimetric analysis confirmed that carboxymethyl chitosan had been successfully anchored on the surface of graphene. In addition, the CMCS-rGO was used as an anticorrosive nanofiller to be added to waterborne epoxy (EP) coatings to protect steel substrates. The corrosion protection behavior of all coatings was tested by electrochemical workstation, and the results proved that the incorporation of well-dispersed CMCS-rGO nanomaterials could significantly improve the anti-corrosion performance of waterborne epoxy coatings. Furthermore,

Journal Pre-proof

even after 180 days of immersion, the impedance modulus value of the 0.2% CMCS-rGO/EP at $|Z|_f$ = 0.01 Hz was still approximately 2 orders of magnitude higher than that of the EP.

Keywords: Carboxymethyl chitosan; Graphene; Anticorrosive; Waterborne epoxy coating

1. Introduction

In recent years, graphene, as a typical two-dimensional (2D) nanomaterial, has attracted considerable attention in the field of corrosion protection, due to its many unique characteristics, such as excellent chemical inertness, outstanding thermal stability and complete impermeability (Böhm, 2014; Dehghani, Bahlakeh, & Ramezanzadeh, 2020; Motamedi, Ramezanzadeh, Ramezanzadeh, & Saadatmandi, 2019). Previous studies have revealed that the anticorrosive performance of metal substrates can be greatly improved by covering a monolayer or a few layers of graphene (Huh et al., 2014). However, recent studies have shown that pinholes, cracks, or scratches on graphene coatings can cause galvanic corrosion between graphene and metals, thereby accelerating metal corrosion (Jo, Lee, Lee, & Cho, 2017; Lee & Berman, 2018).

As an alternative to pure graphene coatings, adding graphene to the polymer matrix is a reasonable way to utilize the properties of graphene for metal protection (Asaldoust, Hosseini, Ramezanzadeh, & Bahlakeh, 2020; Javidparvar, Naderi, & Ramezanzadeh, 2019b; Khalili Dermani, Kowsari, Ramezanzadeh, & Amini, 2019; Ramezanzadeh, Mahdavian, & Bahlakeh, 2020). However, the hydrophobicity of graphene limits its dispersibility in water. In addition, the strong interlayer forces between adjacent nanosheets often causes graphene to aggregate in the polymer matrix, which seriously hinders the application of graphene (Hayatgheib, Ramezanzadeh, Kardar, & Mahdavian, 2018; Picot et al., 2017; Zhang et al., 2020). Hitherto, covalent and non-covalent methods are commonly used to improve the

Journal Pre-proof

water dispersibility of graphene and the compatibility between graphene and polymer matrix (Habibiyan, Ramezanzadeh, Mahdavian, Bahlakeh, & Kasaeian, 2020; Javidparvar, Naderi, & Ramezanzadeh, 2019a; Wang et al., 2019). Ramezanzadeh et al. (2020) synthesized a polyamidoamine dendrimer covalently functionalized graphene oxide nanosheet (GO-PAMAM), which can significantly enhance the corrosion resistance of the epoxy coatings. Zhou et al. (2019) fabricated nanocomposite anticorrosive coatings by incorporating natural amino acids (lysine) chemically covalently modified GO (LY-GO) into waterborne epoxy coatings. The results showed the LY-GO to be well dispersed in waterborne epoxy resins and could improve the anti-corrosion performance of the waterborne epoxy resin coatings. Although chemical covalent modification can improve the dispersion of graphene in the polymer matrix, it tends to introduce defects in the structures of graphene, which will destroy its barrier properties (Ding, Rahman, Peng, Dou, & Yu, 2018; Wang et al., 2019). The non-covalent methods are regarded as an effective strategy because they could maintain the structural integrity of graphene and have a negligible impact on its performance (Chen et al., 2017; Yang, Cao, Li, Rana, & Zhu, 2013; Ye et al., 2019). Wang et al. (2019) used the hydroxyl lignin to exfoliate graphene in aqueous solution, and demonstrated that the addition of lignin-OH functionalized graphene could significantly improve the corrosion resistance of waterborne epoxy coatings. Qiu et al. (2017) prepared a polypyrrole non-covalently functionalized graphene with excellent dispersibility in aqueous solution with significantly enhanced protection ability of waterborne epoxy coating on carbon steel.

Chitosan (CS), as a member of natural polysaccharide family, has numerous advantages such as excellent film-forming properties, non-toxicity, biodegradability, biocompatibility and antibacterial activities (Ashassi-Sorkhabi & Kazempour, 2020; Fayyad, Sadasivuni, Ponnamma, & Al-Maadeed, 2016). Furthermore, CS is also considered as potential green and smart corrosion inhibitor due to its high complexing ability with metal ions and the versatile chemical functionalization (Luckachan &

Journal Pre-proof

Mittal, 2015). Fayyad et al. (2016) has reported an oleic acid-modified chitosan-graphene oxide (OACS/GO) composite coating. The electrochemical impedance spectroscopy (EIS) results show that the corrosion resistance of the OACS/GO coating is improved by 100 times compared with the CS coating. However, CS is only soluble in aqueous solutions under acid conditions, which limits its application in some fields (Anitha et al., 2009). Carboxymethyl chitosan (CMCS), as a derivative of CS, has properties of antibacterial, anticancer and antioxidant, making it a promising candidate in various fields such as tissue engineering, bioimaging, wound healing, drug/enzyme delivery, cosmetics and corrosion inhibitor (Ashassi-Sorkhabi & Kazempour, 2020; Shariatinia, 2018; Upadhyaya, Singh, Agarwal, & Tewari, 2013). In particular, CMCS has excellent water solubility and can be applied to match aqueous anti-corrosion systems (Macedo, Marques, Tonholo, & Balaban, 2019). Eduok et al. (2018) synthesized a water-soluble poly(N-vinyl imidazole) grafted carboxymethyl chitosan (CMCS-g-PVI) as corrosion inhibitor for protecting API X70 in 1.0 M HCl solution. The results showed CMCS-g-PVI to have a better corrosion inhibition effect even at a concentration lower than chitosan. Sun et al. (2018) compared the capabilities of chitosan and carboxymethyl chitosan as corrosion inhibitors in wastewater and found the inhibition efficiency of carboxymethyl chitosan (38%) to be higher than that of chitosan (23%). According to previous research (Pan et al., 2016; Yang, Cao, Li, Rana, & Zhu, 2013), CMCS-functionalized graphene (CMCS-G) composite materials can obtain good water dispersibility, and are expected to be applied in the field of biomedicine. As far as we know, there are few reports on CMCS-functionalized graphene (CMCS-G) composite materials in the field of corrosion protection, especially in the CMCS-G/polymer composite waterborne coating system.

In this work, we propose a facile and efficient method to prepare non-covalently functionalized graphene nanosheets with CMCS to improve the dispersion of graphene nanosheets in waterborne epoxy coatings. The prepared CMCS-rGO/EP was

Journal Pre-proof

used as a corrosion protection layer for steel substrates and analyzed by electrochemical impedance spectroscopy (EIS).

2. Experimental

2.1 Materials

Graphene oxide (GO) was purchased from Suzhou Hengqiu Technology Co. Ltd, China. N-carboxymethyl chitosan (CMCS, molecular weight = 1×10^5 - 2×10^5 g/mol, degree of carboxylation ≥ 80%, CAS: 83512-85-0) was acquired from Macklin Biochemical Co., Ltd. (Shanghai, China). Hydrazine hydrate was purchased from Guangzhou Chemical Reagent Factory, China. Waterborne curing agent (F0705, solid content is 44%) and waterborne epoxy resin (F0704, solid content is 50%) were provided by Shenzhen Jitian Chemical Co., Ltd, China. Deionized water was in all the experiments.

2.2 Preparation of the CMCS-rGO

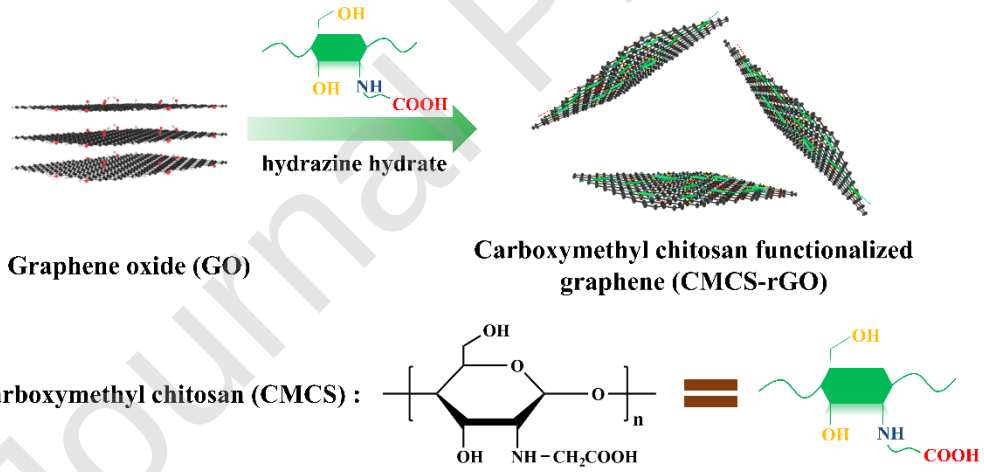

Scheme 1 The preparation of carboxymethyl chitosan functionalized graphene **(**CMCS-rGO).

The preparation procedure of CMCS–rGO was similar to previous research with a modification (Yang, Cao, Li, Rana, & Zhu, 2013). Typically, 0.2 g CMCS was

Journal Pre-proof

slowly dissolved in 100 ml water for 2 h to form a homogeneous solution. Subsequently, a certain amount of GO was dispersed in water via ultrasonication for 1 h to obtain a homogeneous GO dispersion (2 mg/ml). Then the GO dispersion (100 ml) was gradually added to the aqueous solution of CMCS. After mixing, 0.2 mL of hydrazine hydrate was added for further treatment and reacted at 90 °C for 1 h. Finally, the CMCS-rGO hybrid nanomaterial was obtained by filtration, washing with water several times, and freeze drying. For comparison, we also synthesized reduced graphene oxide (rGO) without CMCS in a similar procedure of CMCS-rGO nanomaterial.

2.3 Preparation of nanocomposite coatings

The CMCS-rGO/EP coatings with 0.05 wt%, 0.1 wt%, 0.2 wt%, 0.3 wt% and 0.5 wt% of CMCS-rGO were prepared according to the following steps. Specifically, CMCS-rGO was added to deionized water (20 mL) and sonicated for 1 h to obtain a homogeneous CMCS-rGO aqueous solution, and then 2 g waterborne hardener was added to the obtained solution to continue sonicating for 10 min. Subsequently, 4 g waterborne epoxy resin was added into the systems and stirred until a homogeneous mixture. The mixtures were painted on the pretreated Q235 steel by a bar coater. Finally, after curing at 50 °C for 72 h, the CMCS-rGO/EP composite coatings with a thickness of approximately 150 μm was prepared. For comparison, the EP composite coating with an addition of 0.2 wt% rGO and pure EP coating were also prepared according to the above method.

2.4 Characterization

Fourier transform infrared (FTIR) was carried out in the range of 400-4000cm^{-1} using TENSOR 27 spectroscopy (Bruker Co., Germany). Raman spectrum was measured on a confocal Renishaw inVia Reflex Raman spectrometer. The ultraviolet visible (UV-vis) spectroscopy (UV-8000, Shanghai Metash Instruments Co. Ltd., China) was utilized to confirm the synthesis of CMCS-rGO. Thermal gravimetric

Journal Pre-proof

analysis (TGA, TG209F3 NETZSCH Germany) measurements were performed under N_2 atmosphere in the temperature range of 35-800 ℃, with a heating rate of 10 ℃/min. Transmission electron microscopy (TEM, Jeol JEM-100SX) was used to observe the morphology of rGO and CMCS-rGO in water. Atomic force microscope (AFM, Seiko SPA-400, Japan) was used to characterize the thickness of CMCS-rGO. Scanning electron microscope (SEM, Hitachi S4800, Japan) was used to observe the morphology of rGO and CMCS-rGO in EP matrix.

The electrochemical behaviors of the coatings immersed 3.5 wt.% NaCl solution were measured by CHI-604E electrochemical workstation equipped with a three-electrode system (Shanghai CH Instruments, China). The platinum sheet electrode, saturated calomel electrode (SCE) and the steel coated coatings were used as counter electrode, reference electrode and working electrode, respectively. The potentiodynamic polarization（Tafel) curve analysis measurement was recorded from cathodic direction to the anodic direction (Eocp ± 500 mV) with the sweep rate of 0.5 mV/s. EIS measurement was carried out in the frequency range from 100 kHz to 10 mHz with a sinusoidal perturbation of 20 mV. EIS results were analyzed using ZsimpWin software.

.

3. Results and discussion

3.1 Characterization of CMCS-rGO

Journal Pre-proof

Journal Pre-proof

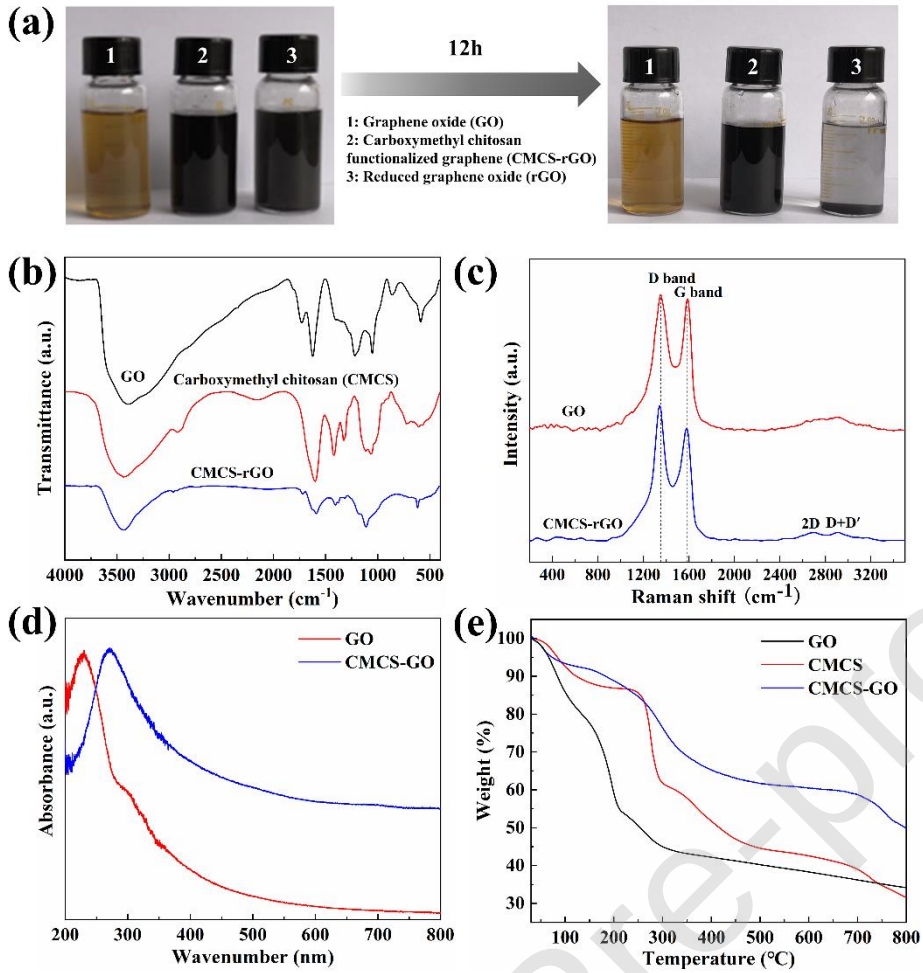

Fig. 1 (a) The dispersion stability of graphene oxide (GO), reduced graphene oxide (rGO) and carboxymethyl chitosan functionalized graphene (CMCS-rGO) in aqueous solution (1mg/ml); (b) FTIR spectra of GO, carboxymethyl chitosan (CMCS) and CMCS-rGO; (c) Raman spectra of GO and CMCS-rGO; (d) UV-vis spectra analyses of GO and CMCS-rGO, both dispersed in water; (e) TGA curves of GO, CMCS and CMCS-rGO.

As shown in Fig. 1(a), after only 1 hour of reaction, a black homogeneous CMCS-rGO aqueous solution was obtained, which was stable over 1 month without any obvious precipitation. In contrast, the rGO aqueous solution without CMCS showed irreversible aggregation and precipitation after only storing for less than 12 hours. The good dispersibility of CMCS-rGO can be attributed to the water solubility of carboxyl groups and the electrostatic repulsion between molecules, which can prevent the internal and internal π–π accumulation of graphene (Yang, Cao, Li, Rana,

Journal Pre-proof

& Zhu, 2013).

FTIR spectra is shown in Fig. 1 (b). Both of CMCS and CMCS-rGO exhibited the basic characteristic peaks of CMCS at 3441 cm^{-1} (O-H stretch), 1591 cm^{-1} (COO^- asymmetry stretching vibration), 1408 cm^{-1} (COO^- symmetric stretching vibration) and 1067 cm^{-1} (C-O absorption peak of secondary hydroxyl group) (Naderi & Azizian, 2018), which indicated that CMCS was successfully adsorbed on graphene. Raman spectrum is shown in Fig.1 (c). GO exhibited two characteristic peaks at 1352 cm^{-1} (D band) and 1587 cm^{-1} (G band), I_D/I_G=1.03. The D band and G band were represented the in-plane vibration of sp^2 carbon atoms and the vibration of sp^3 carbon atoms from the functional groups, respectively (Liu, Kuila, Kim, Ku, & Lee, 2013; Yang et al., 2019). After modification with CMCS, the D band and G band of CMCS-rGO shifted to 1341 cm^{-1} and 1578 cm^{-1}, respectively. Moreover, the I_D/I_G ratio increased significantly from 1.03 for GO to 1.20 for CMCS-rGO, suggesting that the removal of oxygen functional groups in CMCS-rGO and the conversion of sp^3 carbon of GO to sp^2 carbon. In the range of 2500–3200 cm^{-1}, the Raman spectrum exhibited two peaks related to 2D and D + D′ bands. Generally, the strong and broad peaks of the 2D and D + D′ bands indicate that the fewer layers of graphene are exfoliated (Sari & Ramezanzadeh, 2020). For GO, the ratios of the peaks related to the 2D and D + D′ bands to the G band were $I_{2D/G}$ = 0.085 and $I_{D+D'/G}$ = 0.10, respectively. For CMCS-rGO, the values of $I_{2D/G}$ and $I_{D+D'/G}$ were slightly reduced to $I_{2D/G}$ = 0.072 and $I_{D+D'/G}$ = 0.073. This may be attributed to the successful non-covalent functionalization of CMCS on the surface of graphene. UV-vis absorption spectrum is shown in Fig. 1(d). For GO, the π→π* transition of C=C bond and the n→π* transition of C=O bond were observed at 230 nm and 307 nm, respectively. For CMC-G, the absorption peak of the π→π* transition shifted to 272 nm, which can be attributed to the recovery of π electron conjugation on the graphene sheets (Kanazawa, Sato, & Sano, 2019). As can be seen from the TGA analysis result of Fig. 1(e), GO was thermally unstable and lost about a 14.1% weight loss at 100 °C, which

is due to the loss of residual water contained in the GO sheets. The major weight loss was observed at 200 °C, presumably assignable to the pyrolysis of the unstable oxygen-containing groups from the surface of GO sheets (Stankovich et al., 2007). In the case of CMCS-rGO, a more gradual and smaller weight loss was exhibited at around 100 °C due to the hydrophobic of rGO. Furthermore, we noted that CMCS-rGO showed a significant weight loss in the range of 230-500 °C corresponding to the pyrolysis of CMCS glycoside units (Sreedhar, Aparna, Sairam, & Hebalkar, 2007). The results indicate that the CMCS deposited on the surface of graphene was about 24.8 wt.%.

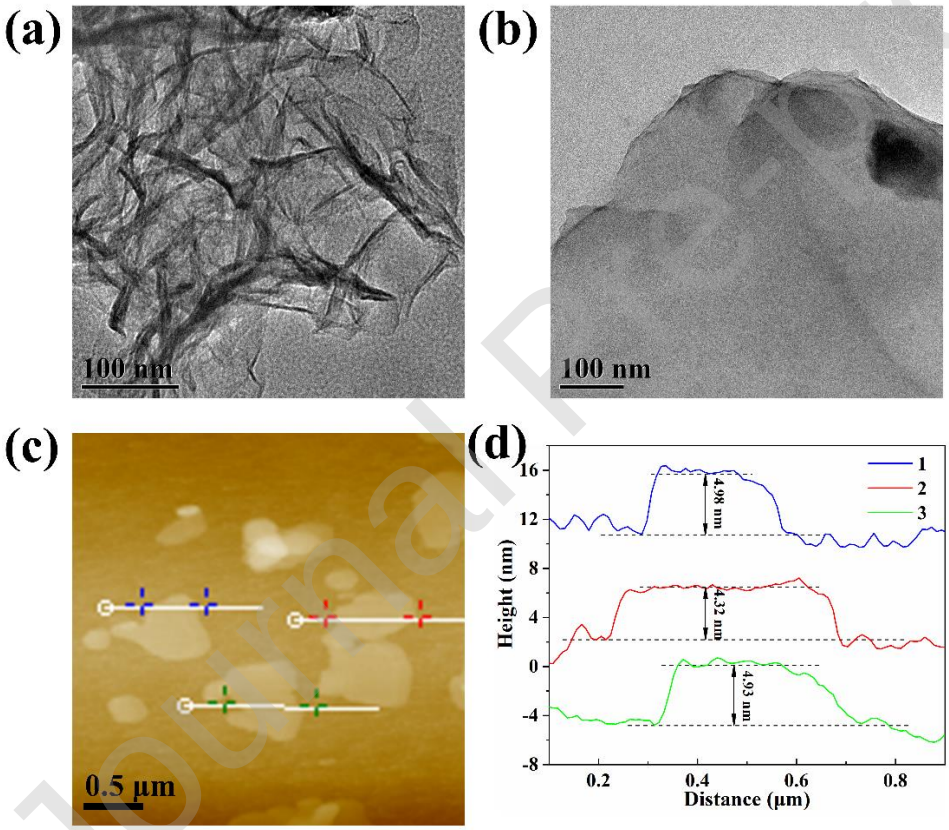

Fig. 2 TEM images of (a) reduced graphene oxide (rGO) and (b) carboxymethyl chitosan functionalized graphene (CMCS-rGO); (c, d) AFM image and corresponding height profile of CMCS-rGO.

As shown in Fig. 2(a), the rGO was showed to be severe aggregation. In

Journal Pre-proof

comparison, the prepared CMCS-rGO was smooth and flat without aggregation, which was attributed to the functionalization of CMCS (Fig. 2(b)). Furthermore, AFM result confirmed the thickness of CMCS-rGO was around 4.32-4.98 nm (Fig. 2(c) and Fig. 2(d)), suggesting the graphene was almost exfoliated to a few layers after functionalization of CMCS.

3.2 Dispersibility of the CMCS-rGO in waterborne epoxy coatings

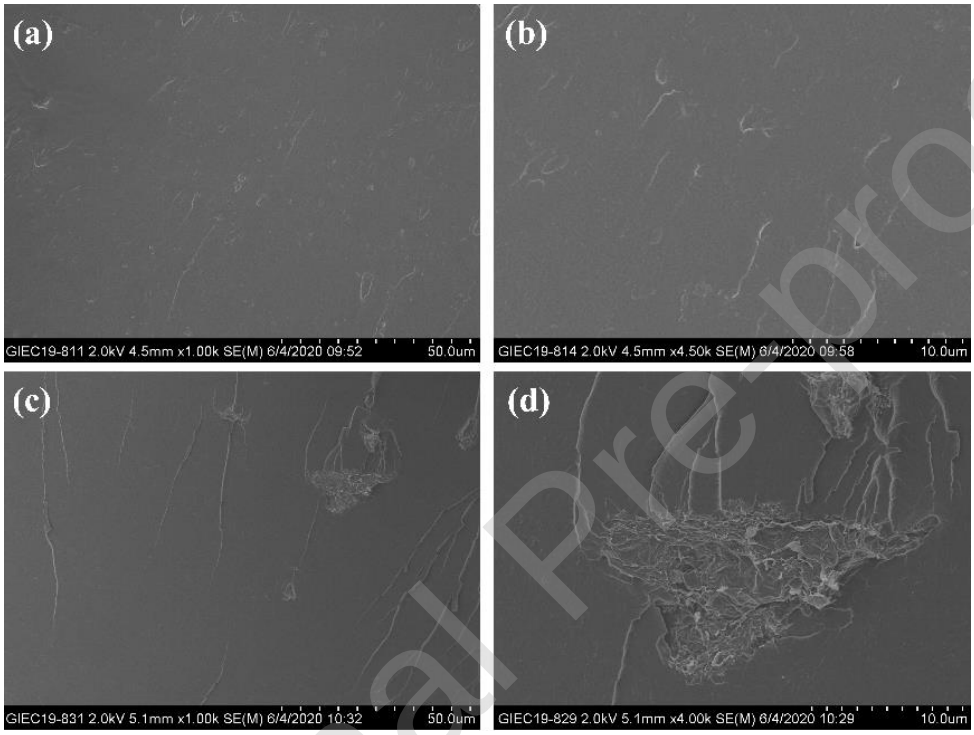

Journal Pre-proof

Journal Pre-proof

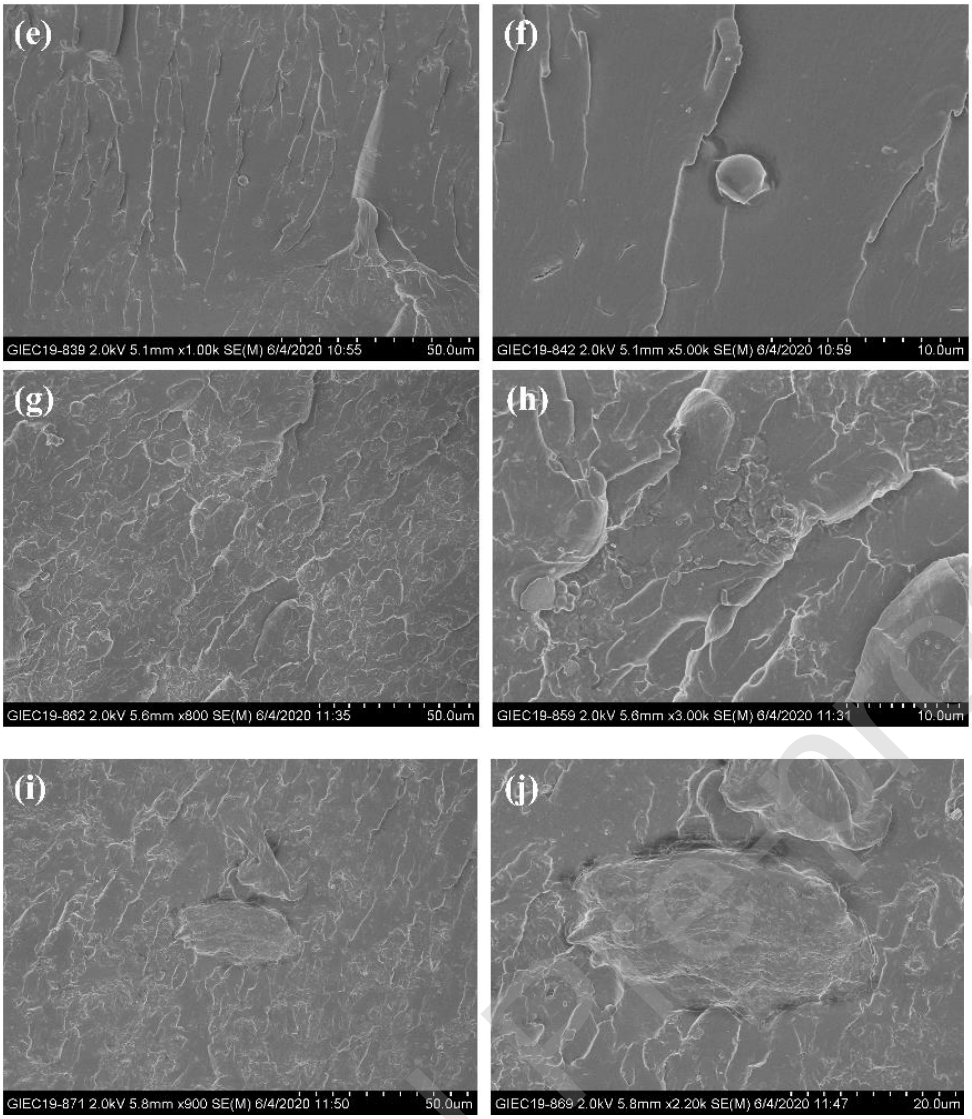

Fig. 3 SEM images of (a, b) pure epoxy resin (EP), (c, d) 0.2% reduced graphene oxide (rGO)/EP, (e, f) 0.05% carboxymethyl chitosan functionalized graphene (CMCS-rGO)/EP, (g, h) 0.2% CMCS-rGO/EP and (i, j) 0.5% CMCS-rGO/EP.

The structure of the fractured surface of EP, rGO/EP and CMCS-rGO nanocomposites were observed by SEM to investigate the dispersion levels of CMCS-rGO nanomaterials in EP matrix. The EP exhibited a relatively clean and smooth fracture surface as shown in Fig. 3(a-b). The fractured surface of 0.2% rGO/EP shown in Fig. 3(c-d) shows obvious aggregation of graphene nanosheets, which indicated poor dispersibility of rGO in EP matrix. However, there was almost no aggregate in the SEM image of 0.2% CMCS-rGO/EP nanocomposite as shown in Fig. 3(g-h). This

Journal Pre-proof

is due to the presence of CMCS on the surface of the CMCS-rGO nanosheets that promoted the interfacial interaction between the graphene nanosheets and the polymer matrix, resulting in the ultrathin CMCS-rGO nanosheets to be uniformly embedded in the EP matrix. In addition, compared to EP and rGO/EP, the fracture surfaces of CMCS-rGO/EP nanocomposites (Fig. 3 (e–j)) displayed more fracture streaks and a rougher surface, and it became more obvious as the amount of CMCS-rGO added increased. This result may be due to the phase separation of graphene nanosheets and waterborne epoxy matrix with an increase in the content of CMCS-rGO (Liu, Qiu, Du, Zhao, & Wang, 2018).

3.3 Corrosion protection performance of coatings

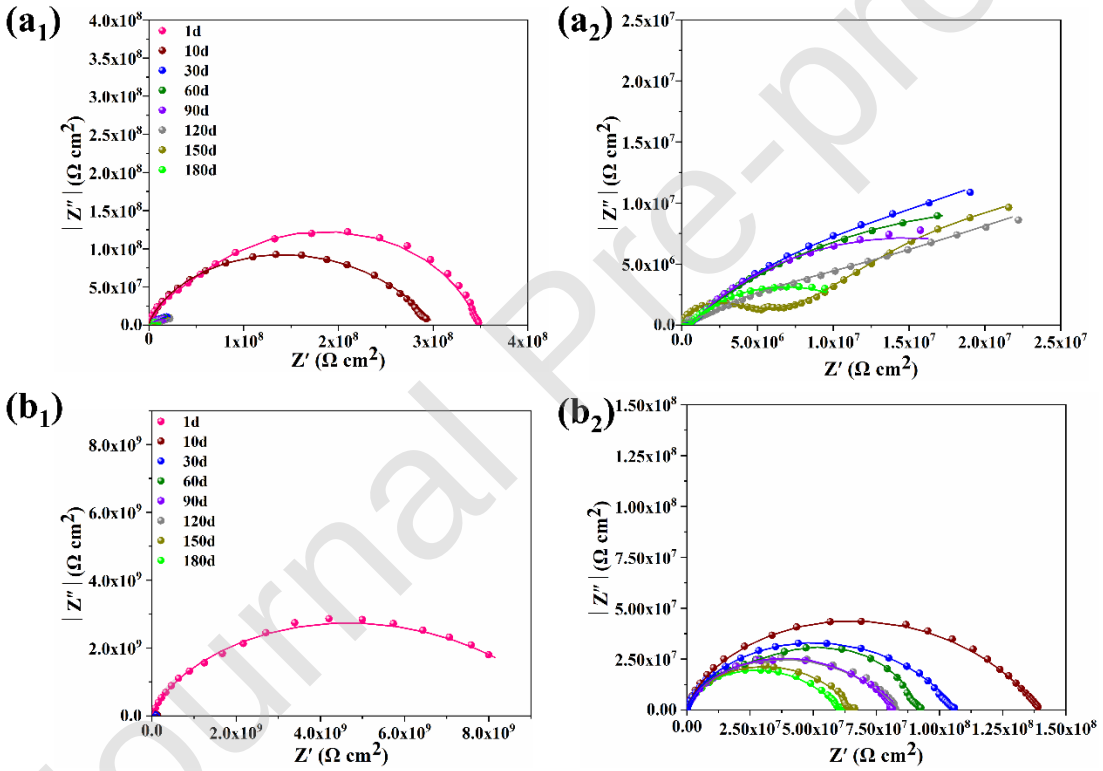

Journal Pre-proof

Journal Pre-proof

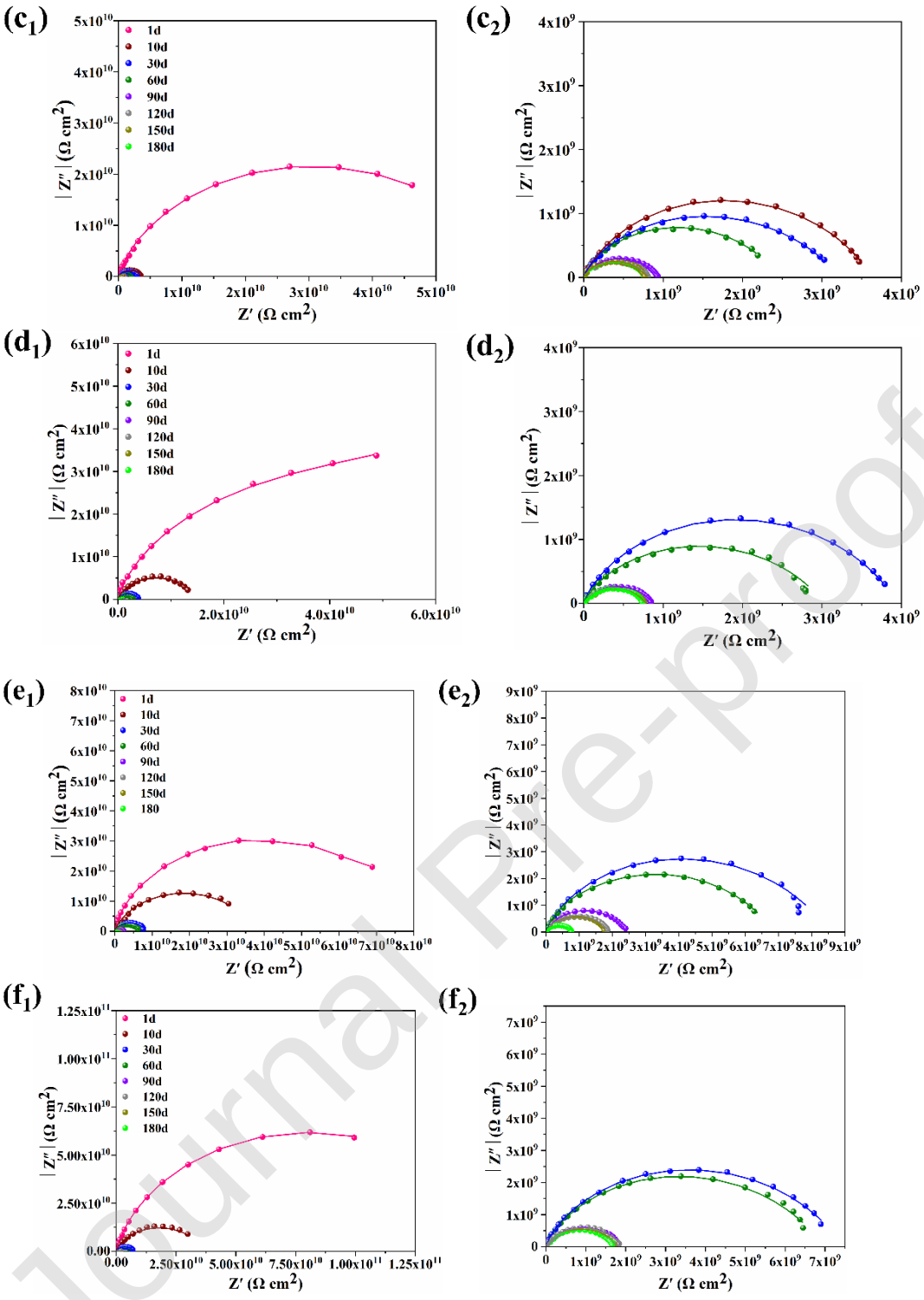

Journal Pre-proof

Journal Pre-proof

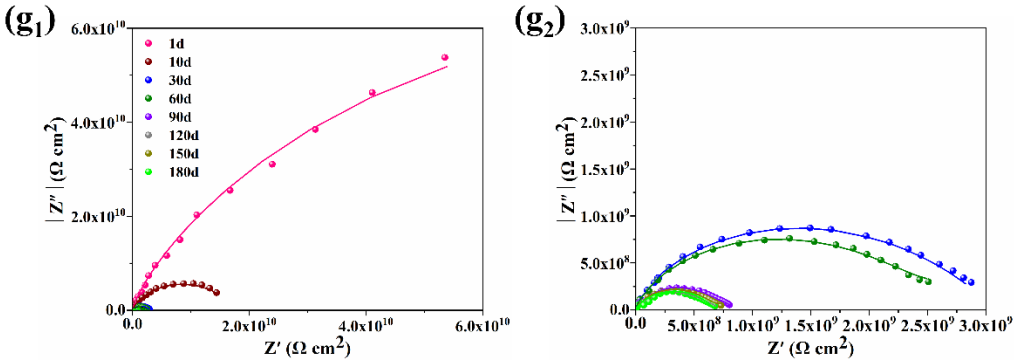

Fig. 4 The Nyquist plots of the nanocomposite coatings after 180 days of immersion in 3.5 wt.% NaCl aqueous solution (a_1)(a_2) pure epoxy resin (EP); (b_1)(b_2) 0.2% reduced graphene oxide (rGO)/EP; (c_1)(c_2) 0.05% carboxymethyl chitosan functionalized graphene (CMCS-rGO)/EP; (d_1)(d_2) 0.1% CMCS-rGO/EP; (e_1)(e_2) 0.2% CMCS-rGO/EP; (f_1)(f_2) 0.3% CMCS-rGO/EP; (g_1)(g_2) 0.5% CMCS-rGO/EP

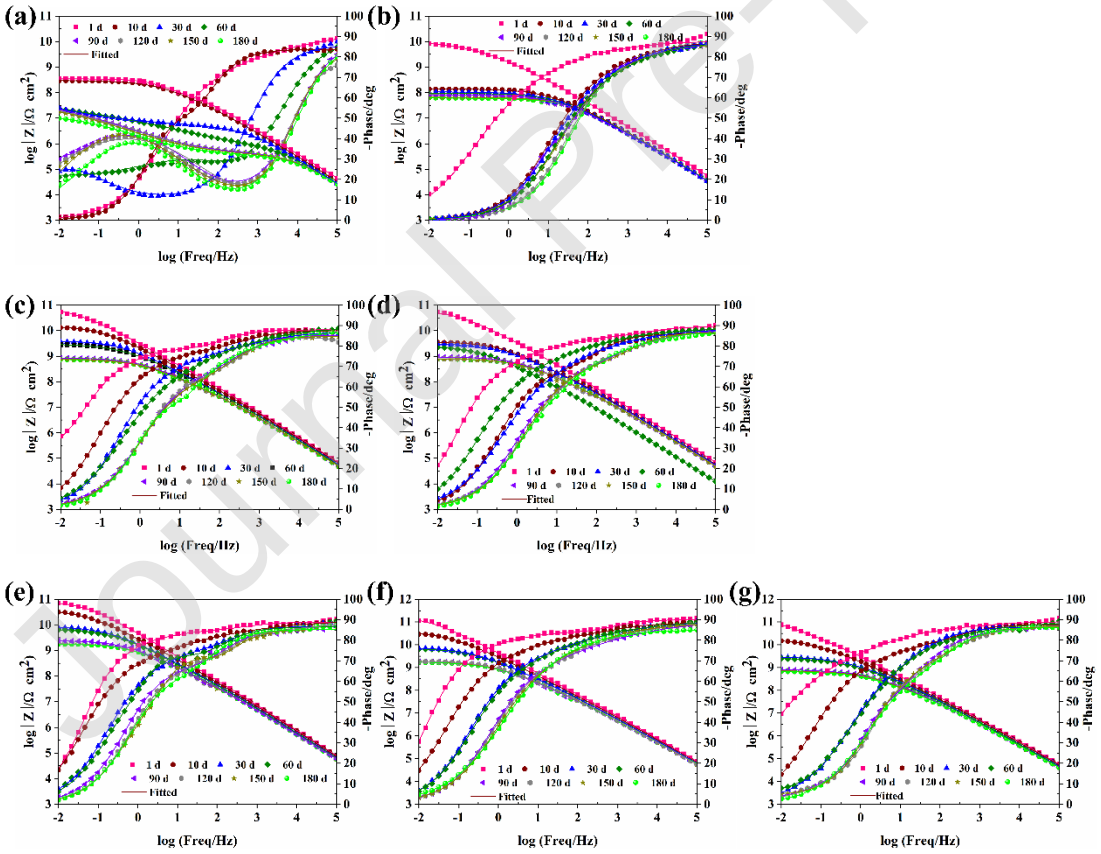

Fig. 5 The Bode plots of the nanocomposite coatings after 180 days of immersion in 3.5 wt.% NaCl aqueous solution (a) pure epoxy resin (EP); (b) 0.2% reduced graphene oxide (rGO)/EP; (c)

Journal Pre-proof

0.05% carboxymethyl chitosan functionalized graphene (CMCS-rGO)/EP; (d) 0.1% CMCS-rGO/EP; (e) 0.2% CMCS-rGO/EP; (f) 0.3% CMCS-rGO/EP; (g) 0.5% CMCS-rGO/EP;

The potentiodynamic polarization curve (Tafel analysis) (Fig. S1 and Table S1) and electrochemical impedance spectroscopy (EIS) measurements were used to investigate the barrier properties and corrosion resistance of the coatings. In the Nyquist plots, a lager diameter capacitive semicircle generally reveals a superior protection performance of the coating (Shi et al., 2020; Zhou et al., 2019). As shown in Fig. 4 (a_1), the capacitance loop of the EP coating continued to shrink, suggesting that the protection of the Q235 steel substrate by the EP coating was gradually failing. In addition, after 30 days of immersion, the capacitance semicircle of EP gradually decreased to a quarter arc (Fig. 4 (a_2)), indicating that the corrosive medium (H_2O, O_2 and Cl^-) had penetrated the coating and corroded the substrate surface (Jorcin, Krawiec, Pébère, & Vignal, 2009; Liu, Qiu, Du, Zhao, & Wang, 2018). The capacitance semicircle diameter of the 0.2% rGO/EP coating was slightly increased compared to the capacitance semicircle diameter of EP as shown in Fig. 4 (b_1) and Fig. 4 (b_2). Although the trend of capacitive arcs in the CMCS-rGO/EP coatings continued to decline, the diameter of the capacitance was much larger than that of EP and rGO/EP coatings and showed a single arc even after immersion for 180 days (Fig. 4 (c-g)). The results implies that the addition of CMCS-rGO could effectively enhance the protection ability of the EP coating on the Q235 substrate.

The impedance modulus plots at a lower frequency ($|Z|_f$ = 0.01 Hz) in the Bode impedance modulus plots can be regarded as an indicator of the barrier performance of the coating (Ramezanzadeh, Niroumandrad, Ahmadi, Mahdavian, & Moghadam, 2016; Shi et al., 2020). As shown in Fig. 5 (a), the initial value of the impedance modulus ($|Z|_f$ = 0.01 Hz) of the EP coating was only 3.46×10^8 Ω cm^2 after immersion for 1 day, and it decreased sharply to 2.34×10^7 Ω cm^2 after immersion for 30 days. The impedance modulus ($|Z|_f$ = 0.01 Hz) of the rGO/EP coating slightly increased as

Journal Pre-proof

shown in Fig. 5 (b), which increased from 9.90×10^{6} Ω cm^2 (EP coating) to 6.16×10^{7} Ω cm^2 (rGO/EP coating) after immersion for 180 days. In addition, it was observed that the impedance modulus values of the CMCS-rGO/EP coatings was much higher than that of the EP and rGO/EP coatings. It can be seen in Fig. 5 (c), the impedance modulus value of the CMCS-rGO/EP coating with only 0.05% CMCS-rGO added after 180 days of immersion remained at 7.43×10^{8} Ω cm^2, which was approximately 2 orders of magnitude higher than that of the EP coating (9.90×10^{6} Ω cm^2). It is particularly worth noting that even after 180 days of immersion, the impedance modulus of the 0.2% CMCS-rGO/EP and 0.3% CMCS-rGO/EP coatings remained at an extremely high value of 1.77×10^{9} Ω cm^2 and 1.74×10^{9} Ω cm^2, respectively. This result may be because the embedding of well dispersed CMCS-rGO could significantly enhance the barrier properties of the EP coating.

The Bode-phase plots was also used to determine the corrosion protection performance of the coating systems as shown in Fig. 5. In general, the phase angle in the frequency range of 10^{-2} to 1 Hz corresponded to the corrosion of the steel substrate, the peaks located at 1 to 10^{3} Hz was attributed to the coating defects, and the phase angle at 10^{4}~10^{5} Hz frequency region was ascribed to the response of the coating. Therefore, it can be concluded that there are many defects in the EP coating substrate as shown in Fig. 5 (a), which quickly fails after immersion for 30 days, and the steel substrate was severely corroded. However, the responses of the corrosion of the steel substrate and the coating defect of the CMCS-rGO/EP coating systems disappeared in the Bode phase plots, and the coating response could be detected in the 10^{1}-10^{5} Hz frequency region. The Bode-phase results revealed that the addition of CMCS-rGO could significantly enhance the corrosion resistance of the EP matrix.

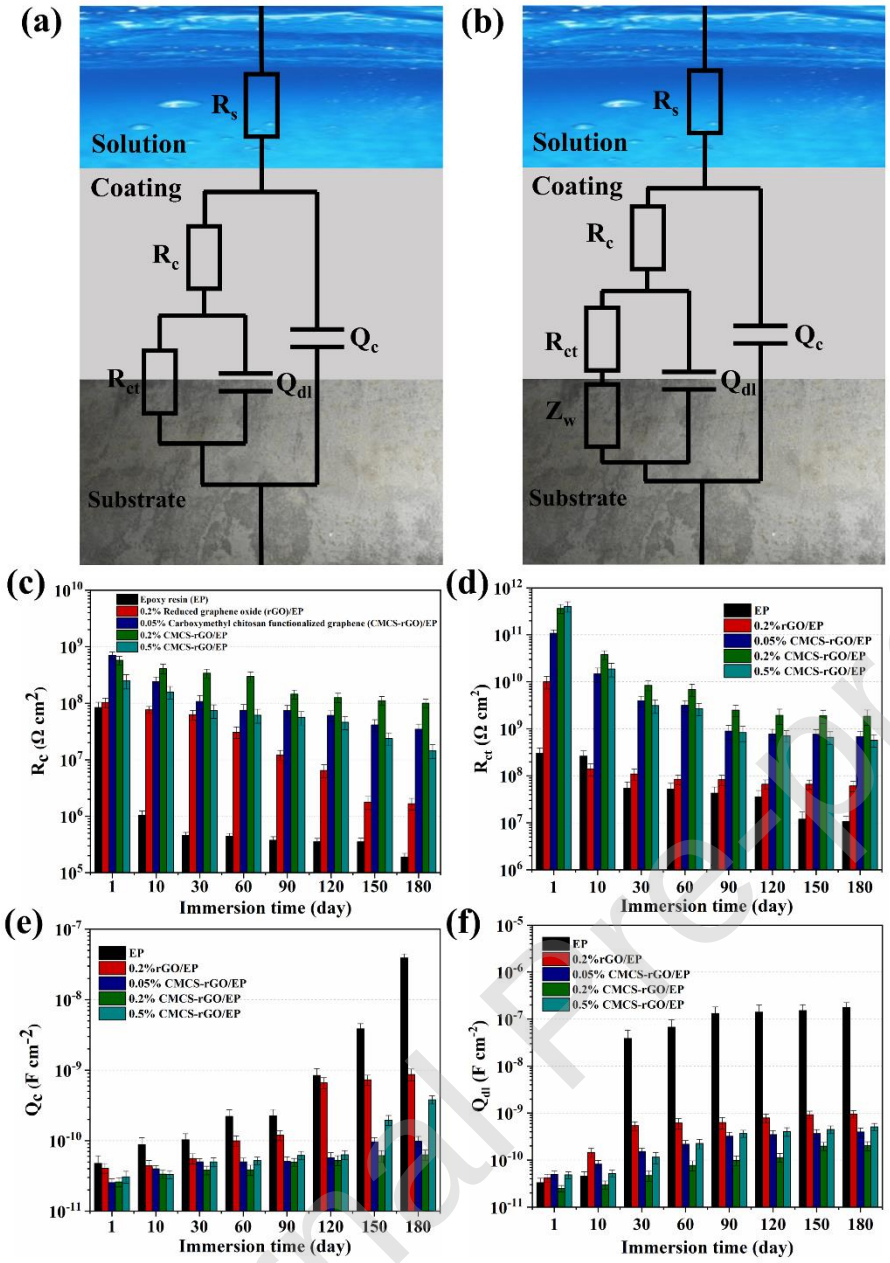

Fig. 6 (a, b) The proposed equivalent electrical circuits for nanocomposite coatings and the fitting results of (c) R_c, (d)R_{ct}, (e) Q_c and (f) Q_{dl} for pure epoxy resin (EP), 0.2% reduced graphene oxide (rGO)/EP and carboxymethyl chitosan functionalized graphene (CMCS-rGO)/EP coatings.

The EIS results of EP, rGO/EP and CMCS-rGO/EP coatings were fitted with the equivalent circuit model using ZSimpWin software and the corresponding electrochemical parameters (Table S2) were obtained to further study the corrosion process. In Fig. 6, R_s was the solution resistance, R_c represents the coating resistance,

Journal Pre-proof

and R_{ct} was defined as the charge transfer resistance. Q_c represents the coating capacitance and Q_{dl} represents the double-layer capacitance. Z_w was the Warburg impedance representing the diffusion of the cathode reaction in the coating (Cui, Ren, Zhao, Xue, & Wang, 2018; Liu, Qiu, Du, Zhao, & Wang, 2018). Compared with solvent-based organic coatings, the 3.5 wt.% NaCl aqueous solution always tended to penetrate water-based coatings and quickly reach saturation (Liu, Du, Zhao, & Wang, 2018; Liu, Qiu, Du, Zhao, & Wang, 2018). In the saturated state, the corrosion control process converted from coating resistance to charge transfer resistance and can be represented by the model of Fig. 6(a). The circuit model of Fig. 6(a) was applied to fit the EP immersed before 30 days, rGO/EP and CMCS-rGO/EP coatings. However, the EP coating detects the diffusion of the cathodic reaction in the coating after being immersed for 30 days and was represented by the circuit model of Fig. 6(b), indicating that the corrosion reaction occurred in the EP coating. The penetration behavior of rGO/EP and CMCS-rGO/EP coatings was successfully suppressed, and the charge transfer process in the coating was still the circuit model of Fig. 6(a). This was attributed to the dispersion of graphene nanosheets in the coating will produce a "labyrinth effect" which can well inhibit the penetration of corrosive media, thereby enhancing the barrier properties of the coating.

It can be clearly observed from Fig. 6(c) that the R_c value of the EP coating dropped sharply from the initial 8.45×10^7 Ω cm^2 to 1.97×10^5 Ω cm^2 after immersion for 180 days. The R_c value of the rGO/EP coating also dropped sharply from the initial 1.03×10^8 Ω cm^2 to 1.67×10^6 Ω cm^2 after immersion for 180 days. Although the R_c values of the CMCS-rGO/EP coating also exhibited a downward trend, the values were always much higher than the R_c values of the EP and rGO/EP coatings. It is worth noting that the R_c value of the 0.2% CMCS-rGO/EP coating (9.98×10^7 Ω cm^2) was still 2~3 orders of magnitude higher than the R_c value of the EP coating even after immersion for 180 days, which reveals that the addition of CMCS-rGO nanosheets can significantly improve the barrier performance of the EP coating. R_{ct}

Journal Pre-proof

was the charge transfer resistance and was inversely proportional to the corrosion rate. As shown in Fig. 6(d), even after 180 days of immersion, the R_{ct} value of the 0.2% CMCS-rGO/EP coating remained at 1.91×10^{9} Ω cm^2, which was about two orders of magnitude higher than that of EP coating (1.08×10^{7} Ω cm^2). This indicates that the electrochemical reaction occurred at the interface between the EP coating and the steel substrate, and this process was significantly suppressed after adding CMCS-rGO. In addition, the coating capacitance Q_c was always used as an indicator of the water resistance of the coating. As shown in Fig. 6(e), it can be seen that the Q_c values of all systems showed an increasing trend with the increase of immersion time. The Q_c value of EP increased from the initial 4.89×10^{-11} F cm^{-2} to 3.93×10^{-8} F cm^{-2} after 180 days of immersion, which was attributed to the high water absorption of the EP coating. For the CMCS-rGO/EP coating, the Q_c values were much lower than that of the EP coating. In particular, the Q_c value of the 0.2% CMCS-rGO/EP coating after 180 days of immersion was 6.37×10^{-11} F cm^{-2}, which was about 3 orders of magnitude lower than that of the EP coating. The Q_{dl} values of all coatings exhibited a similar trend to the Q_c values as shown in Fig. 6(f). Moreover, the 0.2% CMCS-rGO/EP coating exhibit the highest R (R_c, R_{ct}) and the lowest Q (Q_c, Q_{dl}) values.

3.4 Proposed anticorrosion mechanism of nanocomposite coatings.

Journal Pre-proof

Journal Pre-proof

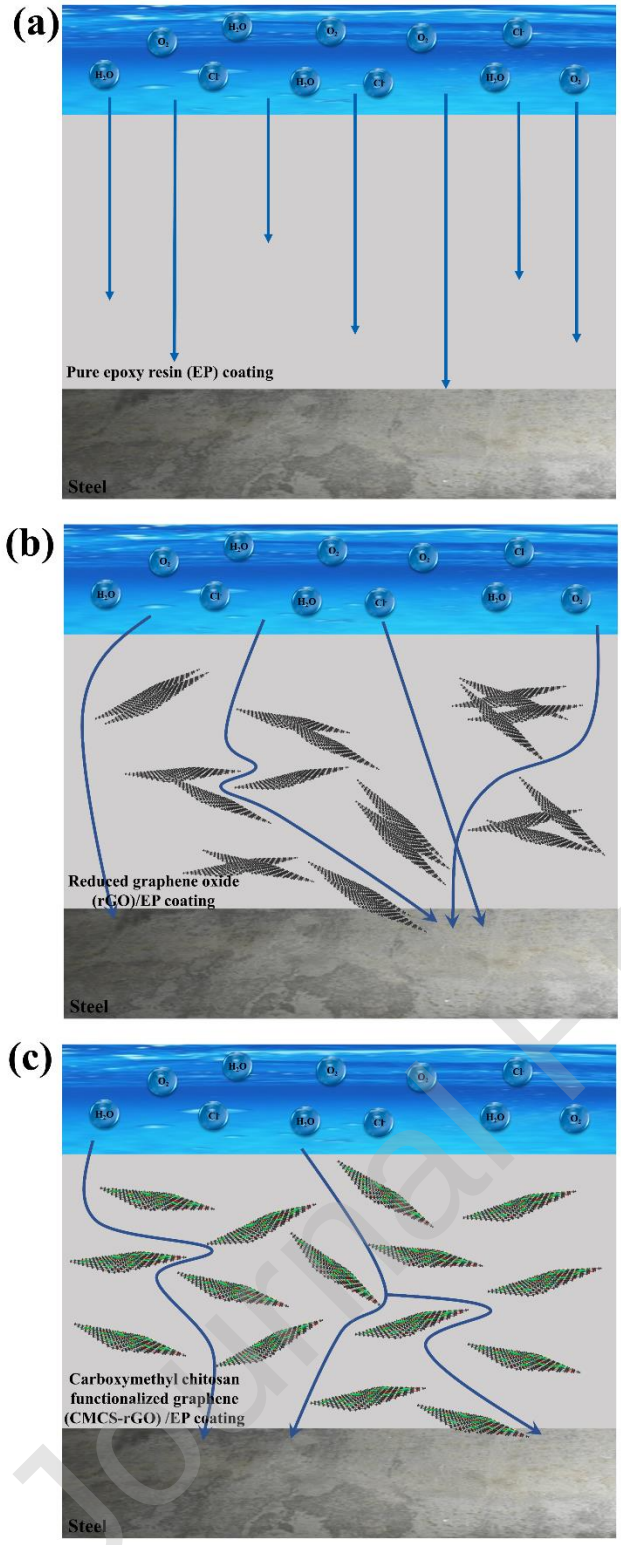

Fig. 7 Proposed anticorrosion mechanism of nanocomposite coatings.

For the traditional EP coating as shown in Fig. 7(a), corrosive media (H_2O, O_2 and Cl^-) would directly pass through the coating to reach the substrate/coating

Journal Pre-proof

interface, resulting in a corrosion reaction. As shown in Fig. 7(b), due to the poor compatibility of rGO with EP matrix, rGO tended to accumulate in the EP matrix, which makes the improvement of the corrosion resistance of the EP coating insignificant. Moreover, once the corrosive medium penetrates, the galvanic corrosion reaction would occur (rGO acts as cathode and steel serves as anode), which would further accelerates the corrosion of the steel substrate (Liu, Du, Zhao, & Wang, 2018). Hence, improving the dispersion of graphene in the EP matrix is a crucial step to enhance the anti-corrosion performance of composite coatings. Coincidentally, carboxymethyl chitosan can help graphene to be well dispersed in the EP matrix. As shown in Fig. 7(c), the well-dispersed CMCS-rGO nanosheets produced a "labyrinth effect" in the EP matrix, providing a more complex diffusion path for corrosive ions, thereby enhancing the corrosion protection performance of the composite coating. Furthermore, loading carboxymethyl chitosan on the surface of graphene can prevent the direct connection of graphene-graphene and graphene-steel, thus inhibiting the occurrence of galvanic corrosion and leading to excellent corrosion resistance.

Conclusions

A non-covalently functionalized graphene with carboxymethyl chitosan was successfully prepared. The results of TEM and SEM revealed that the non-covalently functionalized graphene of CMCS could effectively prevent the aggregation of graphene nanosheets, thereby uniformly dispersing in the waterborne epoxy matrix. In addition, the successfully prepared CMCS-rGO was also incorporated into waterborne epoxy coating to investigate its anti-corrosion properties. The results of Tafel and EIS demonstrated that the incorporation of well-dispersed CMCS-rGO nanomaterials could significantly improve the anti-corrosion performance of waterborne epoxy coatings and protect steel substrates against corrosion. This nanocomposite coating prepared by adding chitosan derivatives to water-based polymers provides an alternative approach for chitosan-based corrosion inhibitor systems, and has excellent

Journal Pre-proof

application prospect in the field of corrosion protection of metal substrates.

Credit Author Statement

Hongyi Shi: Writing - Original Draft, Writing - Review & Editing, Methodology

Weiqu Liu: Supervision, Project administration

Yankun Xie: Resources, Formal analysis

Maiping Yang: Investigation, Data curation

Chunhua Liu: Data curation

Fengyuan Zhang: Resources

Shuo Wang: Validation

Liyan Liang: Supervision, Project administration

Ke Pi: Investigation

Acknowledgements

This study was funded by Guangzhou Institute of Chemistry, Chinese Academy of Sciences, the Guangzhou Science and Technology Plan Project (No. 201707010274, 201904010244).

Journal Pre-proof

Journal Pre-proof

References

Anitha, A., et al. (2009). Synthesis, characterization, cytotoxicity and antibacterial studies of chitosan, O-carboxymethyl and N,O-carboxymethyl chitosan nanoparticles. *Carbohydrate Polymers,* 78(4), 672-677.

Asaldoust, S., Hosseini, M. S., Ramezanzadeh, B., & Bahlakeh, G. (2020). Construction of a unique anti-corrosion nanocomposite based on graphene oxide@Zn_3PO_4/epoxy; experimental characterization and detailed-theoretical quantum mechanics (QM) investigations. *Construction and Building Materials,* 256.

Ashassi-Sorkhabi, H., & Kazempour, A. (2020). Chitosan, its derivatives and composites with superior potentials for the corrosion protection of steel alloys: a comprehensive review. *Carbohydrate Polymers,* 237, 116110.

Böhm, S. (2014). Graphene against corrosion. *Nature Nanotechnology,* 9(10), 741-742.

Chen, C., et al. (2017). Achieving high performance corrosion and wear resistant epoxy coatings via incorporation of noncovalent functionalized graphene. *Carbon,* 114, 356-366.

Cui, M., Ren, S., Zhao, H., Xue, Q., & Wang, L. (2018). Polydopamine coated graphene oxide for anticorrosive reinforcement of water-borne epoxy coating. *Chemical Engineering Journal,* 335, 255-266.

Dehghani, A., Bahlakeh, G., & Ramezanzadeh, B. (2020). Designing a novel targeted-release nano-container based on the silanized graphene oxide decorated with cerium acetylacetonate loaded beta-cyclodextrin (β-CD-CeA-MGO) for epoxy anti-corrosion coating. *Chemical Engineering Journal,* 400.

Ding, J., Rahman, O. U., Peng, W., Dou, H., & Yu, H. (2018). A novel hydroxyl epoxy phosphate monomer enhancing the anticorrosive performance of waterborne graphene/epoxy coatings. *Applied Surface Science,* 427, 981-991.

Eduok, U., Ohaeri, E., & Szpunar, J. (2018). Electrochemical and surface analyses of X70 steel corrosion in simulated acid pickling medium: Effect of poly (N-vinyl imidazole) grafted carboxymethyl chitosan additive. *Electrochimica Acta,* 278, 302-312.

Fayyad, E. M., Sadasivuni, K. K., Ponnamma, D., & Al-Maadeed, M. A. A. (2016). Oleic acid-grafted chitosan/graphene oxide composite coating for corrosion protection of carbon steel. *Carbohydrate Polymers,* 151, 871-878.

Habibiyan, A., Ramezanzadeh, B., Mahdavian, M., Bahlakeh, G., & Kasaeian, M. (2020). Rational assembly of mussel-inspired polydopamine (PDA)-Zn (II) complex nanospheres on graphene oxide framework tailored for robust self-healing anti-corrosion coatings application. *Chemical Engineering Journal,* 391.

Hayatgheib, Y., Ramezanzadeh, B., Kardar, P., & Mahdavian, M. (2018). A comparative study on fabrication of a highly effective corrosion protective system based on graphene oxide-polyaniline nanofibers/epoxy composite. *Corrosion Science,* 133, 358-373.

Journal Pre-proof

Huh, J. H., et al. (2014). Enhancement of seawater corrosion resistance in copper using acetone-derived graphene coating. *Nanoscale,* 6(8), 4379-4386.

Javidparvar, A. A., Naderi, R., & Ramezanzadeh, B. (2019a). Designing a potent anti-corrosion system based on graphene oxide nanosheets non-covalently modified with cerium/benzimidazole for selective delivery of corrosion inhibitors on steel in NaCl media. *Journal of Molecular Liquids,* 284, 415-430.

Javidparvar, A. A., Naderi, R., & Ramezanzadeh, B. (2019b). Epoxy-polyamide nanocomposite coating with graphene oxide as cerium nanocontainer generating effective dual active/barrier corrosion protection. *Composites Part B: Engineering,* 172, 363-375.

Jo, M., Lee, H. C., Lee, S. G., & Cho, K. (2017). Graphene as a metal passivation layer: Corrosion-accelerator and inhibitor. *Carbon,* 116, 232-239.

Jorcin, J.-B., Krawiec, H., Pébère, N., & Vignal, V. (2009). Comparison of local electrochemical impedance measurements derived from bi-electrode and microcapillary techniques. *Electrochimica Acta,* 54(24), 5775-5781.

Kanazawa, K., Sato, H., & Sano, M. (2019). Reaction kinetics of reducing graphene oxide at individual sheet level studied by twilight fluorescence microscopy. *The Journal of Physical Chemistry C,* 123(11), 6881-6887.

Khalili Dermani, A., Kowsari, E., Ramezanzadeh, B., & Amini, R. (2019). Utilizing imidazole based ionic liquid as an environmentally friendly process for enhancement of the epoxy coating/graphene oxide composite corrosion resistance. *Journal of Industrial and Engineering Chemistry,* 79, 353-363.

Lee, J., & Berman, D. (2018). Inhibitor or promoter: insights on the corrosion evolution in a graphene protected surface. *Carbon,* 126, 225-231.

Liu, C., Du, P., Zhao, H., & Wang, L. (2018). Synthesis of l-histidine-attached graphene nanomaterials and their application for steel protection. *ACS Applied Nano Materials,* 1(3), 1385-1395.

Liu, C., Qiu, S., Du, P., Zhao, H., & Wang, L. (2018). An ionic liquid-graphene oxide hybrid nanomaterial: synthesis and anticorrosive applications. *Nanoscale,* 10(17), 8115-8124.

Liu, H., Kuila, T., Kim, N. H., Ku, B.-C., & Lee, J. H. (2013). *In situ* synthesis of the reduced graphene oxide–polyethyleneimine composite and its gas barrier properties. *Journal of Materials Chemistry A,* 1(11).

Luckachan, G. E., & Mittal, V. (2015). Anti-corrosion behavior of layer by layer coatings of cross-linked chitosan and poly(vinyl butyral) on carbon steel. *Cellulose,* 22(5), 3275-3290.

Macedo, R., Marques, N. D. N., Tonholo, J., & Balaban, R. C. (2019). Water-soluble carboxymethylchitosan used as corrosion inhibitor for carbon steel in saline medium. *Carbohydrate Polymers,* 205, 371-376.

Motamedi, M., Ramezanzadeh, M., Ramezanzadeh, B., & Saadatmandi, S. (2019). Enhancement of the active/passive anti-corrosion properties of epoxy coating via inclusion of histamine/zinc modified/reduced graphene oxide nanosheets. *Applied*

Journal Pre-proof

Surface Science, 488, 77-91.

Naderi, Z., & Azizian, J. (2018). Synthesis and characterization of carboxymethyl chitosan/Fe_3O_4 and $MnFe_2O_4$ nanocomposites hydrogels for loading and release of curcumin. *Journal of Photochemistry and Photobiology B,* 185, 206-214.

Pan, Q., et al. (2016). Lactobionic acid and carboxymethyl chitosan functionalized graphene oxide nanocomposites as targeted anticancer drug delivery systems. *Carbohydrate Polymers,* 151, 812-820.

Picot, O. T., et al. (2017). Using graphene networks to build bioinspired self-monitoring ceramics. *Nature Communications,* 8, 14425.

Qiu, S., Li, W., Zheng, W., Zhao, H., & Wang, L. (2017). Synergistic effect of polypyrrole-intercalated graphene for enhanced corrosion protection of aqueous coating in 3.5% NaCl solution. *ACS Appl Mater Interfaces,* 9(39), 34294-34304.

Ramezanzadeh, B., Niroumandrad, S., Ahmadi, A., Mahdavian, M., & Moghadam, M. H. M. (2016). Enhancement of barrier and corrosion protection performance of an epoxy coating through wet transfer of amino functionalized graphene oxide. *Corrosion Science,* 103, 283-304.

Ramezanzadeh, M., Ramezanzadeh, B., Mahdavian, M., & Bahlakeh, G. (2020). Development of metal-organic framework (MOF) decorated graphene oxide nanoplatforms for anti-corrosion epoxy coatings. *Carbon,* 161, 231-251.

Ramezanzadeh, M., Ramezanzadeh, B., Sari, M. G., & Saeb, M. R. (2020). Corrosion resistance of epoxy coating on mild steel through polyamidoamine dendrimer-covalently functionalized graphene oxide nanosheets. *Journal of Industrial and Engineering Chemistry,* 82, 290-302.

Sari, M. G., & Ramezanzadeh, B. (2020). Epoxy composite coating corrosion protection properties reinforcement through the addition of hydroxyl-terminated hyperbranched polyamide non-covalently assembled graphene oxide platforms. *Construction and Building Materials,* 234.

Shariatinia, Z. (2018). Carboxymethyl chitosan: properties and biomedical applications. *International Journal of Biolological Macromolecules,* 120(Pt B), 1406-1419.

Shi, H., et al. (2020). Polyethylenimine-assisted exfoliation of h-BN in aqueous media for anticorrosive reinforcement of waterborne epoxy coating. *Progress in Organic Coatings,* 142.

Sreedhar, B., Aparna, Y., Sairam, M., & Hebalkar, N. (2007). Preparation and characterization of HAP/carboxymethyl chitosan nanocomposites. *Journal of Applied Polymer Science,* 105(2), 928-934.

Stankovich, S., et al. (2007). Synthesis of graphene-based nanosheets via chemical reduction of exfoliated graphite oxide. *Carbon,* 45(7), 1558-1565.

Sun, H., Wang, H., Wang, H., & Yan, Q. (2018). Enhanced removal of heavy metals from electroplating wastewater through electrocoagulation using carboxymethyl chitosan as corrosion inhibitor for steel anode. *Environmental Science:*

Journal Pre-proof

Water Research & Technology, 4(8), 1105-1113.

Upadhyaya, L., Singh, J., Agarwal, V., & Tewari, R. P. (2013). Biomedical applications of carboxymethyl chitosans. *Carbohydrate Polymers*, 91(1), 452-466.

Wang, S., et al. (2019). Green synthesis of graphene with the assistance of modified lignin and its application in anticorrosive waterborne epoxy coatings. *Applied Surface Science*, 484, 759-770.

Yang, G., Cao, J., Li, L., Rana, R. K., & Zhu, J.-J. (2013). Carboxymethyl chitosan-functionalized graphene for label-free electrochemical cytosensing. *Carbon*, 51, 124-133.

Yang, J. H., et al. (2019). Improving radio frequency transmission properties of graphene via carrier concentration control toward high frequency transmission line applications. *Advanced Functional Materials*, 29(18).

Ye, Y., et al. (2019). Superior corrosion resistance and self-healable epoxy coating pigmented with silanzied trianiline-intercalated graphene. *Carbon*, 142, 164-176.

Zhang, X., et al. (2020). A powder-metallurgy-based strategy toward three-dimensional graphene-like network for reinforcing copper matrix composites. *Nature Communications*, 11(1), 2775.

Zhou, X., et al. (2019). Facile modification of graphene oxide with lysine for improving anti-corrosion performances of water-borne epoxy coatings. *Progress in Organic Coatings*, 136.

Journal Pre-proof